

Photochemical control of endogenous ion channels and cellular excitability

Doris L. Fortin¹, Matthew R. Banghart², Timothy W. Dunn¹, Katharine Borges¹, Daniel A. Wagenaar³, Quentin Gaudry³, Movses H. Karakossian⁴, Thomas S. Otis⁴, William B. Kristan³, Dirk Trauner^{2*}, and Richard H. Kramer^{1*}

¹Department of Molecular and Cell Biology, University of California Berkeley, 121 Life Sciences Addition, Berkeley, CA 94720-3200 and ²Department of Chemistry, University of California Berkeley, Latimer Hall, Berkeley, CA 94720-1460. ³Department of Biology, University of California San Diego, 9500 Gilman Drive, La Jolla, CA 92037-0357. ⁴Department of Neurobiology, University of California, Los Angeles, 63-314 CHS Box 951763, Los Angeles, CA 90095-1763.

*To whom correspondence should be addressed. E-mail: trauner@berkeley.edu; rhkramer@berkeley.edu

ABSTRACT

Light-activated ion channels provide a precise and non-invasive optical means for controlling action potential firing, but the genes encoding these channels must first be delivered and expressed in target cells. Here we describe a method for bestowing light sensitivity onto endogenous ion channels that does not rely on exogenous gene expression. The method utilizes a synthetic photoisomerizable small molecule, or Photoswitchable Affinity Label (PAL), that specifically targets K⁺ channels. PALs contain a reactive electrophile, enabling covalent attachment of the photoswitch to naturally occurring nucleophiles in K⁺ channels. Ion flow through PAL-modified channels is turned on or off by photoisomerizing PAL with different wavelengths of light. We show that PAL treatment confers light sensitivity onto endogenous K⁺ channels in isolated neurons and intact neural structures, allowing rapid optical regulation of excitability without genetic modification.

INTRODUCTION

Eukaryotic cells possess ion channels that are directly activated by voltage or ligands, but not by light. Consequently, electrical or chemical stimuli are often used to elicit physiological responses in excitable cells. However, light stimulation has several advantages over electrodes or chemical perfusion devices. Light is non-invasive and can be projected on tissue with great temporal and spatial precision. It can be focused on subcellular structures, single cells, or projected diffusely to regulate the activity of many cells simultaneously¹⁻⁵. But how can light be used to manipulate the activity of “blind” cells that have no natural photoresponsive proteins?

One popular approach to manipulate the activity of excitable cells with light has been to use a “caged” neurotransmitter (for example glutamate) that is liberated from a photolabile protecting group (the cage) upon exposure to light^{1,5}. Photorelease of caged glutamate accurately mimics the kinetics of synaptic transmission and has been used to map neuronal circuits⁶⁻⁹. However, glutamate uncaging is ill-suited for inducing sustained activity because prolonged uncaging can lead to the accumulation of desensitized receptors and local depletion of the caged neurotransmitter⁴. Photorelease is irreversible and diffusion of the liberated neurotransmitter can result in unintended activation of receptors on untargeted cells.

To circumvent the limitations associated with using a freely diffusible light sensitive compound, several types of light-activated proteins have been used to control neuronal activity. A light-activated K⁺ channel (SPARK), consisting of a photoswitchable ligand attached to a genetically engineered Shaker K⁺ channel, allows reversible suppression of action potential firing¹⁰. LiGluR, a light-activated glutamate receptor, containing a different photoswitchable ligand attached to a genetically engineered iGluR⁶¹¹, reversibly depolarizes cells and promotes neuronal firing¹². Finally, channelrhodopsin-2 (ChR2) and halorhodopsin (NpHR), which use the natural photoswitch retinal, allow light to trigger or inhibit action potential firing¹³⁻¹⁹. Each of these proteins can impart light sensitivity on neuronal firing, but only if their gene is first introduced into the cell of interest and the protein expressed in sufficient abundance on the plasma membrane. However, exogenous expression of proteins can be non-uniform and slow, requiring days to weeks, and is not currently practical in some organisms. Genes encoding light-activated

proteins can also be introduced transgenically into organisms^{12,19-22} but this may perturb the development and function of cells expressing the genes.

Here we describe a new method, based on a Photoswitchable Affinity Label (PAL), to confer light sensitivity to proteins without requiring genetic engineering and exogenous gene expression. Consequently, the PAL approach can be used to photosensitize endogenous proteins and control their activity in freshly obtained, genetically unadulterated cells or tissues. The PAL molecules described here specifically target voltage-gated K⁺ channels and act as covalently tethered channel blockers. Appropriate design of other PAL molecules however, should allow the approach to be extended to other ligand-responsive proteins at the cell surface. The tether is photoisomerizable and can be shortened or elongated by exposure to different wavelengths of light, allowing or disallowing the blocking moiety to reach the pore. When applied to neurons, PAL enables control of endogenous K⁺ channels with light, resulting in optical control of electrical excitability without genetic modification.

RESULTS

The PAL approach

PALs are derivatives of the photoisomerizable molecule azobenzene (AZO; **Fig. 1a**). Connected to one end of AZO is a protein-binding ligand, in this case a quaternary ammonium group (QA), which binds to the pore of K⁺ channels and blocks ion conduction. On the other end is an electrophilic group (R) that covalently tethers the photoswitch to the channel. We have designed PALs with three different electrophilic groups, acrylamide (AAQ), chloroacetamide (CAQ) or epoxide (EAQ) (**Fig. 1b**; see **supplementary methods** for synthesis) to enable attachment to nucleophilic amino acid side chains. Binding of the QA to the K⁺ channel pore promotes attachment of these PALs if the channel possesses a nucleophile at ~20 Å from the QA binding site, matching the length of the PAL molecule. Hence, the covalent attachment of PALs to channels is promoted by ligand binding, as in classical affinity labeling²³. After the photoswitch is tethered, the QA can reach the pore and block ion conduction only when the AZO is in its elongated *trans* form, but not in its bent *cis* form (**Fig. 1c**). Thus, channels are unblocked by exposure to 360-400 nm light, which photoisomerizes the AZO from *trans* to *cis*. The reverse

cis to *trans* conversion, which restores channel block, occurs slowly in the dark ($\tau = \sim 5$ minutes) and is accelerated by long wavelength light (450-560 nm)^{10,24}.

PAL-modified channels differ in several ways from the previously described SPARK channel¹⁰. SPARK is based on a Shaker K⁺ channel engineered to contain an extracellular cysteine that serves as the covalent attachment site for its photoswitch (**Fig. 1d**). Additional mutations were introduced in the channel to shift voltage-dependent activation and minimize inactivation. The SPARK photoswitch is maleimide-AZO-QA (MAQ, **Fig. 1b**), which covalently attaches to the channel via a maleimide group often considered selective for cysteines. Thus, to impart light sensitivity using SPARK, two components must be added, the channel gene and the MAQ photoswitch. In contrast, the PAL photoswitch acts on endogenous K⁺ channels that have no introduced cysteine and no mutations to modify gating. Hence PAL is a one-component system for conferring light sensitivity.

PAL imparts light sensitivity to K⁺ channels

We assessed the feasibility of the PAL approach using whole-cell patch clamp recording in cells heterologously expressing Shaker K⁺ channels. First, we engineered an appropriately positioned nucleophilic site in Shaker (E422C) to maximize the probability of attachment of the PAL photoswitch to the channel. Addition of AAQ to Shaker E422C photosensitized this channel, enabling regulation of ion flow with light (**Fig. 2a**). Importantly, AAQ also imparted light sensitivity to a Shaker channel lacking the cysteine substitution (E422; **Fig. 2b**) and indeed, conferred a similar degree of light sensitivity on a Shaker channel devoid of extracellular cysteines (data not shown). The fraction of current that could be photoregulated after AAQ treatment (% photoswitching) was similar for E422C and E422 Shaker channels ($77 \pm 15\%$ and $83 \pm 11\%$ respectively, $n = 4$ cells; **Fig. 2c**). CAQ and EAQ also photosensitized E422 Shaker (data not shown). Hence, PAL molecules can find a covalent attachment site at an appropriate distance from the channel pore, such that light-elicited changes in photoswitch length allow or disallow block by the QA group. PAL-modified channels could be photoswitched repeatedly with little decrement in the fraction of current regulated and no apparent photobleaching of the photoswitch (**Fig. 2a** and **b**). Thus, PAL molecules can be used to endow persistent light sensitivity to a wild-type Shaker channel, allowing rapid and reversible control of channel

function.

If PAL molecules can impart light sensitivity on wild-type Shaker, perhaps they can also act on other QA-sensitive K⁺ channels. We expressed various channels in HEK293 cells and quantified photosensitivity after AAQ treatment (**Fig. 2c**). Several K⁺ channels became light sensitive, including Kv1.2, Kv1.3, Kv1.4, Kv2.1 and Kv4.2 (% photoswitching for Kv1.2, $76 \pm 16\%$; Kv1.3, $93 \pm 9\%$; Kv1.4, $90 \pm 13\%$; Kv2.1, $89 \pm 5\%$; Kv4.2, $69 \pm 4\%$; n = 4 cells each; Fig. 2c). Light sensitivity was less pronounced for Kv3.3 ($25 \pm 13\%$ photoswitching, n = 5 cells) and BK ($24 \pm 13\%$ photoswitching, n = 4 cells). In contrast, Kv3.1 exhibited no detectable photosensitivity after AAQ treatment ($2 \pm 6\%$ photoswitching, n = 6 cells). Moreover, neither voltage-gated Na⁺ channels (Nav1.2) nor voltage-gated Ca²⁺ channels (L-type) became light sensitive after AAQ treatment ($1 \pm 5\%$ and $-2 \pm 5\%$ photoswitching respectively, n = 4-7 cells).

PAL photosensitizes K⁺ channels in cultured neurons

We next tested whether PAL molecules could photosensitize endogenous K⁺ channels in neurons. Endogenous voltage-gated K⁺ channels set the resting membrane potential and the threshold for triggering action potentials. They also shape the action potential waveform and regulate the propensity to fire repetitively in response to a stimulus. We recorded voltage-gated outward K⁺ currents from cultured hippocampal neurons before and after AAQ application. Steady-state I-V curves indicate that AAQ application and exposure to 500 nm light blocked a large fraction of voltage-gated K⁺ currents (**Fig. 3a and b**; average current blocked $72 \pm 9\%$, n = 5). Photoisomerization of AAQ to its *cis* configuration with 380 nm light completely relieved K⁺ channel block such that the I-V curve overlapped with that before AAQ treatment (**Fig. 3a and b**; average current recovered under 380 nm, $117 \pm 29\%$, n = 5). Voltage-gated K⁺ currents were photoswitched to a similar extent in neurons treated with CAQ (data not shown). In contrast, MAQ failed to impart light sensitivity on endogenous neuronal K⁺ channels (**Fig. 3c**; $88 \pm 5\%$ and $2 \pm 13\%$ photoswitching for AAQ and MAQ respectively, n = 6 each).

In darkness, the PAL photoswitch will relax to its *trans* configuration, blocking PAL-modified K⁺ channels and potentially causing depolarization of the membrane potential. To prevent tonic blockade of K⁺ channels, 380 nm light can be used to keep PAL-modified channels unblocked

(**Fig. 3a and b**). However, because the spontaneous *cis* to *trans* isomerization of the photoswitch occurs over many minutes in the dark¹⁰, flashes of 380 nm light (1 second per minute) were sufficient to maintain $94 \pm 4\%$ of the K⁺ current unblocked in AAQ-treated neurons (n = 10). Thus, the state of PAL-modified K⁺ channels can be set with the appropriate illumination conditions, preventing tonic K⁺ channel blockade.

Despite having a reactive electrophile and causing K⁺ channel blockade in darkness and 500 nm light, PAL photoswitches did not have obvious deleterious effects on cultured hippocampal neurons. Neurons remained active with a normal resting membrane potential (vehicle, -54 ± 13 mV, n = 10; AAQ, -54 ± 13 mV, n = 23; p > 0.1 unpaired *t*-test) and normal membrane resistance (vehicle, 77 ± 20 M Ω , n = 10; AAQ, 113 ± 65 M Ω , n = 6; p > 0.1 unpaired *t*-test) for several hours after PAL treatment. Further, there was no significant difference in cell death between neurons treated for 15 minutes with vehicle alone ($5 \pm 3\%$), AAQ ($9 \pm 3\%$) or CAQ ($8 \pm 3\%$; n = 4-8 fields each, p > 0.05; One-way ANOVA; **Supplementary Fig. 1**). EAQ appeared more toxic and was not used further in our studies ($25 \pm 11\%$ cell death). Similar results were obtained after treatment for 60 minutes, 4-times longer than needed to impart light sensitivity (**Supplementary Fig. 1**). We also tested neurons up to 6 days after a 15 minute treatment with AAQ and found no significant toxicity ($3 \pm 1\%$ cell death) compared to treatment with vehicle alone ($4 \pm 1\%$). Additional experiments showed that AAQ injection into the vitreous humor of the rat eye successfully imparted light sensitivity onto retinal ganglion cells (RGCs), but had no effect on either the histology of the retina or on the rod- and cone-driven light response, as measured in electroretinogram recordings (Borges and Kramer, unpublished observations). Hence, at least for our treatment conditions, AAQ does not appear toxic to neurons *in vitro* or *in vivo*.

Like other light-activated ion channels, optical control of PAL-modified K⁺ channels can alter the frequency of action potential firing in treated neurons. To allow reliable measurement of photoregulation of firing frequency, we induced continuous firing by injecting depolarizing current in AAQ-treated neurons exposed to 500 nm light. Subsequent photoisomerization of AAQ with 380 nm light, which unblocks K⁺ channels, rapidly suppressed action potential firing (**Fig. 4a**). High-frequency firing resumed upon continuous illumination with 500 nm light. In

addition, flashes of 500 nm light followed by darkness resulted in sustained firing that long outlived the light stimulus (**Fig. 4b**), reflecting the stability of the photoswitch in its *trans* configuration. Hence, light flashes of either wavelength are sufficient to toggle on and off channel blockade and neuronal excitability, eliminating the need for continuous illumination. This feature differentiates PAL-mediated control from regulation by glutamate uncaging and ChR2, which generally affects neurons only during the illumination period. The persistent nature of PAL photoisomers after brief illumination minimizes potential photodamage both to the photoswitch and to target cells by reducing the total amount of light required for optical control. Photocontrol of PAL-modified channels with continuous or intermittent light occurred rapidly, resulting in modulation of neuronal firing within hundreds of milliseconds after the onset of illumination, with the exact delay varying with light intensity. We also found that the afterhyperpolarization at the end of the action potential was more pronounced in 380 nm than 500 nm light, consistent with K⁺ channel regulation (**Fig. 4c**).

Unlike other light-activated channels, PAL targets native ion channels that control cellular excitability, thereby altering the threshold for action potential firing. Current injections that failed to elicit action potential firing under 380 nm light reliably induced firing when a neuron was illuminated with 500 nm light (**Fig. 5a**). The relative proportion of *cis* and *trans* photoisomers of azobenzene-containing photoswitches is dependent on wavelength^{10,24}. This photoequilibrium can be exploited to adjust the extent of K⁺ channel block in a graded manner to fine-tune cellular excitability. Thus, the amount of depolarizing current required to induce action potential firing decreased as the number of blocked K⁺ channels was increased with longer wavelengths (**Fig. 5b**). Photoregulation of voltage-gated K⁺ channels also allows control of spike frequency adaptation. Neurons responding to depolarizing current injection with a single spike in 380 nm light fired repetitively when illuminated with visible light (400-500 nm; **Fig. 5c**) and the frequency of firing was graded depending on the wavelength of illumination (**Fig. 5d**). Photoregulation of AAQ-modified channels thus modulates firing threshold (i.e. rheobase) as well as the number of action potentials fired in response to a given current injection (**Fig. 5e**).

Targeted photosensitivity with optical imprinting

Channel modification by AAQ is dependent on the presence of a nucleophile at the correct

distance from the QA binding site. We have shown that covalent attachment occurs when cells are treated in the dark with AAQ in its extended *trans* form. However, the reactive moiety of PAL will encounter different amino acids when the photoswitch is in its shorter *cis* configuration. To test whether AAQ can attach to K⁺ channels in its *cis* form, we applied it while illuminating a subpopulation of neurons with 380 nm light (**Fig. 6a**). The remaining neurons were kept in darkness and thus were exposed to AAQ in its *trans* form. Neurons illuminated with 380 nm light during PAL treatment showed little photosensitivity, whereas those kept in darkness exhibited light-regulated K⁺ currents (**Fig. 6b, c and d**; treatment in 380 nm light, $5 \pm 5\%$ photoswitching, $n = 10$; treatment in darkness, $54 \pm 16\%$ photoswitching, $n = 9$). The magnitude of the unblocked K⁺ current in the two groups of cells was not significantly different ($3,515 \pm 1022$ pA, $n = 9$ and $4,355 \pm 1466$ pA respectively, $n = 10$; $p > 0.1$, Student's unpaired *t*-test). Hence, photosensitization of K⁺ channels by PAL is itself sensitive to light. This feature can be exploited to pre-program specific cells to become light sensitive by employing selective illumination during PAL treatment.

PAL-mediated optical control of activity in neural tissue

So far, we have shown that PAL molecules enable optical control of cells in culture. For the approach to be effective in tissue, the only additional requirement is that the photoswitch and light reach the cells of interest. We evaluated PAL-mediated optical control of neuronal firing in freshly obtained rat cerebellar slices. After pretreatment with AAQ, we recorded from cerebellar basket cells using the loose-patch configuration. Recordings were obtained in the presence of AMPA, NMDA, and GABA_A receptor antagonists, leaving the basket cells synaptically isolated from the rest of the circuit. Blocking AAQ-modified K⁺ channels with 500 nm light promoted the firing of basket cells while unblocking channels with 360 nm light decreased their firing (**Fig. 7a**; Photoregulation was observed in 6/6 basket cells in AAQ-treated slices and 0/8 basket cells in untreated slices). These results demonstrate that the penetration of AAQ and the delivery of light are not significantly impeded in brain tissue.

We next tested AAQ on the medicinal leech *Hirudo medicinalis*, a system in which the introduction of foreign genes required for other types of light-activated proteins is not widely used. Specifically, we obtained extracellular recordings from the heart central pattern generator

(CPG) interneurons (HN cells). HN cells control the contraction of the heart by bursting in alternation and imposing this rhythm on heart motor neurons. The neuropeptide FMRFamide decreases the burst period of HN cells, possibly by modulating voltage-gated K⁺ currents²⁵. By allowing specific and reversible photoregulation of K⁺ channels, the PAL approach provides a means to assess the contribution of K⁺ channels in the bursting pattern of HN cells. We found that unblocking AAQ-modified K⁺ channels with 380 nm light decreased burst period of HN cells while 500 nm light extended the period (**Fig. 7b**, n = 4 pairs). This is consistent with modeling studies that predict changes in HN cell burst pattern upon modulation of K⁺ channels²⁶. The ability to photoregulate neurons in the leech heartbeat CPG demonstrates that the PAL approach is a powerful method to control K⁺ channels and electrical activity in an intact neural circuit without genetic modification.

The installation of light sensitivity on neurons may enable the artificial input of information downstream from sites of damage or degeneration. For example, the loss of visual function caused by degeneration of rods and cones could be alleviated by treatments that impart light sensitivity on downstream neurons that are normally light insensitive. We tested whether PAL treatment could impart light sensitivity on RGCs, which relay information from the retina to the brain. Loose-patch recordings obtained from RGCs after AAQ treatment showed that their firing increased in 500 nm light and decreased in 380 nm light (**Fig. 7c**), owing to the block and unblock of AAQ-modified K⁺ channels. Robust photocontrol of firing was observed in 15/23 RGCs in AAQ-treated retina and 0/10 RGCs in non-AAQ-treated retina. The retina contains a small fraction of RGCs (~2.5%) that express melanopsin and are intrinsically photosensitive²⁷, but it is unlikely that these cells account for the AAQ results reported here.

DISCUSSION

Here we describe a new set of chemical tools for the optical control of endogenous K⁺ channels and neuronal excitability based on photoswitchable affinity labels (PALs). Traditional affinity labels consist of a ligand that covalently attaches to its target protein via a reactive group. Affinity labels have been used to identify amino acids involved in ligand binding as well as to map distances between selected residues and a ligand binding site in a variety of proteins.

Affinity labels can cause permanent activation or inhibition of protein function since covalent attachment results in persistent occupancy of the ligand binding site²³. We have expanded on the affinity labeling concept by including a photoisomerizable azobenzene linker between the ligand and the reactive group, enabling photoregulation of ligand occupancy and protein function. By using the pore-blocking QA as the ligand, we have designed PALs selective for K⁺ channels. The inclusion of a promiscuous reactive group resulted in covalent attachment and photoregulation of several types of K⁺ channels, but not Na⁺ and Ca²⁺ channels, presumably because labeling is selective for channels that have a QA binding site. The modular nature of PALs enables easy modification of each functional group in the molecule, yielding a combinatorial toolkit for optical regulation of endogenous proteins. For instance, the reactive group could be altered to enable selective attachment to particular amino acids or protein sequences and the photoisomerizable moiety modified to alter the spectral sensitivity or photoswitching kinetics. Finally, inclusion of the appropriate ligand should target PAL molecules to particular types of ion channels and receptors, allowing optical control of a variety of physiological functions.

Genetically encoded light-activated proteins, such as ChR2, LiGluR, SPARK, and NpHR, have emerged as potent tools for mapping microcircuitry because their expression can be restricted to subpopulations of neurons. In contrast, PAL molecules target intrinsic cellular proteins and thus impart photosensitivity on all treated cells, as long as they express the photoswitch target. Widespread photosensitivity may facilitate functional analysis of processes that involve the coordinated firing of multiple cells. However, if regulation of particular cells is desired, there are three ways to restrict PAL-mediated photocontrol. First, PAL can be applied locally so that only a restricted cell or group of cells becomes photosensitized. Second, local illumination can be used during treatment to optically imprint PAL and thus photosensitize particular cells. Third, after PAL treatment, light of the appropriate wavelength can be projected locally to regulate excitability in individual cells or groups of cells. The key asset of the PAL approach is that long-term light sensitivity can be installed onto freshly obtained tissue, unadulterated by exogenous gene expression and possible developmental consequences of ectopic protein expression.

ChR2 and LiGluR are effective tools for driving precise spike trains in neurons^{12-14,16,17} because

they encode non-specific cation channels that directly lead to membrane depolarization. In contrast, the molecular targets of PAL are voltage-gated K⁺ channels, which act as a “brake” rather than a direct trigger of activity. Thus, although light flashes can induce action potential firing in PAL-treated neurons, the temporal fidelity is lower than with other light-activated ion channels that directly depolarize the membrane. Instead, the strength of PAL lies in its persistent and effective control over excitability, which enables light to modulate neuronal firing reversibly. Moreover, because photoisomerization can be controlled bi-directionally, the level of cellular excitability can be titrated by controlling the equilibrium between *cis* and *trans* photoisomers using different wavelengths of light. Although the isomerization of azobenzene-containing photoswitches occurs over a broad range of wavelengths (*cis*: 360-400nm; *trans*: 450-560nm), wavelengths longer than 560 nm do not affect the photoswitch^{10,24}. Thus, it may be possible to combine PAL-mediated optical control with imaging of activity-dependent fluorescent dyes to generate an all-optical system for controlling and recording neuronal excitability.

The distinct mechanism of action of PAL explains why it is particularly effective in controlling the activity of neurons that are spontaneously active; their voltage-gated K⁺ channels are continually opening and therefore continuously subject to optical regulation with PAL. But in theory, PAL should allow modulation of excitability even in quiescent neurons when they are receiving depolarizing input. More complex features of excitability, such as action potential firing threshold and spike frequency adaptation, can also be rendered light sensitive using PAL. In addition, AAQ treatment allows optical neuromodulation of pacemaker activity in the leech heartbeat CPG, mimicking the actions of a neuropeptide. Voltage-gated K⁺ channels participate in the control of excitability in a large number of cell types and thus play a crucial role in the regulation of neuronal communication, endocrine and exocrine secretion, cardiac signaling and vascular contraction. By enabling photocontrol of endogenous K⁺ channels, the PAL approach provides a powerful means to control these physiological functions with light.

Because it targets endogenous proteins the PAL approach is applicable to systems in which introduction of foreign genes is impractical or difficult. Indeed, it is conceivable that modified PAL molecules might ultimately be useful for imparting optical control of neurons in humans,

without requiring gene therapy. A particularly relevant tissue for PAL-mediated optical regulation is the retina, the sole part of the nervous system that is exposed to light *in vivo*. Our data show that AAQ confers light-sensitivity onto RGCs that are not intrinsically light sensitive, raising the possibility that PAL treatment, along with an appropriate optical system, may be used as an alternative to multielectrode-based retinal prosthetic devices²⁸ to restore visual function in retinas with damaged or degenerated rod and cone photoreceptors.

ACKNOWLEDGEMENTS

We thank E. Isacoff, J. Chambers, S.-Y. Choi and S. Jackman for helpful comments, J. Flannery and K. Greenberg for help with RGC experiments, D. Johnston, (University of Texas at Austin) B. Rothberg (University of Texas Health Science Center at San Antonio), B. Rudy (New York University), W. Catterall (University of Washington) and J. Trimmer (University of California Davis) for providing plasmids. This work was supported by the Howard Hughes Medical Institute (KB), the National Science Foundation (IOB-BSC to WBK), Microsoft Research Labs (WBK) and the National Institutes of Health (GM057027 to DT, MH43396 to WBK, and EY16249 to RHK). DAW, QG and WBK thank A. Blankenship and M. Feller for the loan of their xenon lamp.

METHODS

Cell culture, plasmids and transfection. HEK293 cells were grown in DMEM containing 5% fetal bovine serum (FBS). For HEK293T cells, 500 $\mu\text{g/ml}$ G-418 was also included. For electrophysiology, cells were plated at 12×10^3 cells/ cm^2 on poly-L-lysine coated coverslips and transfected using the calcium phosphate method²⁹. The Shaker H4 used here contained the $\Delta 6-46$ deletion to minimize fast inactivation³⁰. Kv4.2 was co-transfected with KCHIP3, at a 4:1 ratio³¹. Recordings were performed 24-48 hours after transfection for K^+ channels and 96 hours for Nav1.2. L-type Ca^{2+} channels currents were recorded from GH3 cells grown in F-12K containing 15% horse serum and 2.5% FBS, 48 hours after plating. Hippocampal neurons were prepared from neonatal rats according to standard procedures³², plated at 50×10^3 cells/ cm^2 on poly-L-lysine coated coverslips and grown in MEM containing 5% FBS, 20 mM glucose, B27 (Invitrogen), glutamine and Mito+ Serum Extender (BD Biosciences). Recordings were performed 14-25 days after plating. Animal care and experimental protocols were approved by the UC Berkeley Animal Care and Use Committee.

PAL treatment. Cells were incubated at 37°C in the dark for 15 minutes with 200-300 μM (hippocampal neurons) or 400 μM (HEK293, HEK293T and GH3 cells) AAQ diluted in bath solution. Cerebellar slices were treated at room temperature in the dark with 200 μM AAQ for 8 minutes. Retinas and leech ganglia were treated with 150 μM and 400 μM AAQ respectively.

Illumination for photoswitching was provided using a xenon lamp (175 W) with narrow band pass filters (380BP10 and 500BP5). Light output was measured using a handheld Newport meter (840-C model). At the back of the objective, light output was 0.3 mW/cm^2 for the 380 nm light and 2.5 mW/cm^2 for the 500 nm light. When measured through a 40X objective and normalized to the focal area at the specimen plane, light output was 0.5 mW/mm^2 and 3.5 mW/mm^2 for the 380 nm and 500 nm light respectively. For some experiments, illumination was provided with a monochromator (TILL Photonics, Polychrome V).

Data analysis. All data reported in the text or shown in bar graphs are averages \pm standard deviation.

Electrophysiological recordings from cultured cells. Recordings were made in the whole-cell patch clamp configuration using pipettes with 3-5 M Ω resistance. To elicit voltage-gated K⁺ currents from neurons and HEK293 cells, holding potential was set to -70 mV and stepped to +30mV for 250 ms. To elicit voltage-gated Na⁺ currents, HEK293T cells expressing Nav1.2 were held at -80 mV and stepped to 0 mV for 250 ms. L-type Ca²⁺ currents were recorded in GH3 cells and elicited by stepping to +20 mV for 200 ms from a holding potential of -40mV. Bath and intracellular solutions compositions are provided in the **supplementary methods**.

Tissue preparation and recordings. Parasagittal cerebellar slices (300 μ m) were prepared from P14-P20 rats using standard techniques approved by the UCLA Animal Care Committee. After sectioning, slices were incubated for 30 minutes at 35 °C in aCSF (composition in **supplementary methods**) then brought to room temperature for PAL treatment and recording. Loose-patch recordings were made in the presence of 6,7-dinitroquinoxaline-2,3-[1*H*,4*H*]-dione, gabazine and [*RS*]-3-[2-carboxypiperazin-4-yl]-propyl-1-phosphonic acid using pipettes with 3-5 M Ω resistance. The depth of recorded basket cells was approximately 25-30 μ m. Retinas were dissected from P50-P60 rats under continuous flow of oxygenated saline solution (composition in **supplementary methods**). Dissected retinas were treated at 37°C with 20 U/ml cysteine-activated papain for 8-20 minutes then washed with saline containing 10 mg/ml BSA and 10 mg/ml trypsin inhibitor followed by PAL treatment and recording using the loose-patch configuration. Dissections and recordings from leech ganglia were conducted as described previously³³. Extracellular signals from heart interneurons (HNs) were obtained using the loose-patch configuration.

Additional methods. Detailed descriptions of the chemical syntheses and the electrophysiology solutions are available in **Supplementary Methods**.

FIGURE LEGENDS

Figure 1. The PAL approach for imparting light sensitivity onto native ion channels

(a) PAL molecules consist of a photoisomerizable azobenzene group (AZO) flanked by a quaternary ammonium (QA; burgundy) and a covalent attachment group (R). Exposure to 380 nm light isomerizes the AZO to its shorter *cis* form whereas exposure to 500 nm light favors the *trans* configuration.

(b) Chemical structure of PAL molecules and MAQ. PAL molecules contain a promiscuous reactive group (orange): acrylamide (Acryl-AZO-QA or AAQ), chloroacetamide (CAQ), or epoxide (EAQ). MAQ contains a maleimide (blue) designed to react with an engineered cysteine.

(c-d) Generation of photoswitch-regulated K⁺ channels. First, QA binds to the channel pore increasing the local concentration of the photoswitch. A PAL molecule covalently attaches via its promiscuous reactive group to an endogenous nucleophile (Nu) on a native K⁺ channel (c). For the SPARK channel, MAQ attaches via its maleimide to a genetically introduced cysteine (E422C) in a Shaker K⁺ channel (d). In both cases, the photoswitch allows control of ionic current using light. In 500 nm light, the photoswitch is extended, blocking ion conduction. In 380 nm light, AZO isomerizes to its *cis* form, retracting the QA and allowing ion conduction. Molecular coordinates from KcsA (PDB ID: 2A9H) were drawn using MacPyMol (DeLano, W.L. The PyMOL Molecular Graphics System (2002); <http://www.pymol.org>).

Figure 2. Photocontrol of K⁺ channels expressed in HEK293 cells

(a) AAQ photosensitizes Shaker channels that contain an engineered nucleophilic attachment site (Sh E422C). Voltage-gated K⁺ currents were elicited by pulsing from -70 to +30 mV for 250 ms. 500 nm light (green) blocks current through the channels whereas 380 nm light (violet) unblocks the channels.

(b) AAQ photosensitizes wild-type Shaker channels (Sh E422). Pulse protocols as in (a).

(c) Percent photoswitching for different channels treated with AAQ (400 μ M, 15 min). We defined percent photoswitching as the difference between the steady-state current in 380 and 500 nm light, divided by the current in 380 nm light. Current was elicited by stepping from -70 to +30 mV (K^+ channels), -80 to 0 mV (Na^+ channels), and -40 to +20 mV (Ca^{2+} channels) (n=4-7 cells for each channel).

Figure 3. Photocontrol of native K^+ current in cultured hippocampal neurons

(a) Steady-state I-V curves from a voltage-clamped hippocampal pyramidal neuron before (Pre; black squares) and after a 15 min application of 300 μ M AAQ in the presence of 500 nm light (green circles) or 380 nm light (violet circles).

(b) AAQ-treated channels are completely unblocked by 380 nm light. Voltage-gated currents (elicited by stepping from -70mV to +30mV) measured after AAQ treatment were normalized to those measured prior to AAQ application (n = 5).

(c) Percent photoswitching for K^+ current in hippocampal neurons treated with AAQ (200 μ M) or MAQ (250 μ M) (n = 6 for each).

Figure 4. Photocontrol of neuronal firing

(a-b) Current clamp recordings from hippocampal neurons treated with AAQ and exposed to different illumination conditions to control firing. Exposure to alternating 380 (violet) and 500 (green) nm light to allow or inhibit action potential firing (a). Exposure to a 200 ms flash of 500 nm light (green) followed by either light of 380 nm (violet) to trigger a transient burst of spikes (b; left) or followed by darkness to trigger sustained activity (b; right). In both (a) and (b) depolarizing current was injected throughout to promote continuous action potential firing.

(c) Current clamp recordings of single action potentials in an AAQ-treated neuron illuminated with 500 nm light (green) or 380 nm light (violet). Action potentials were induced with 500 ms depolarizing current injection (120 pA in 380 nm light, 100 pA in 500 nm light).

Figure 5. Modulation of neuronal excitability with light

(a) Effect of PAL treatment on the current threshold for eliciting action potentials in hippocampal neurons. Identical current pulses (250 pA, 50 ms; 5 Hz) that fail to induce spikes in 380 nm light, reliably elicit spikes in 500 nm light.

(b) Effect of different wavelengths of light on voltage-gated K⁺ channel blockade and action potential threshold. Neurons treated with PAL were exposed to increasing wavelengths of light. For each wavelength, the percent maximal block of voltage-gated K⁺ current (blue, n = 5 cells) was compared to the current injection threshold required to fire a spike (red, n = 6 cells).

(c) Effect of different wavelengths of light on spike frequency adaptation. Current injection (300 pA, 1s) in neurons treated with PAL was performed during exposure to 380 nm, 400 nm, 420 nm or 500 nm light, eliciting different firing patterns.

(d) Relationship between illumination wavelength and average spike frequency during depolarizing pulses (n = 9 cells).

(e) Effect of illumination wavelength on firing threshold and sensitivity to current injection. Neurons were treated with PAL and then exposed to progressively greater current injections under 380 nm or 500 nm illumination. Currents were normalized to the maximal amount of current injected in each cell. Current injections lasted 500 ms and ranged from 15 to 360 pA. (n = 6 cells)

Figure 6. Local illumination during PAL treatment imprints photosensitivity onto specific neurons

(a) Illustration of experimental setup. A hippocampal neuronal culture was uniformly exposed to 300 μM AAQ. During treatment, the microscope objective was used to illuminate a subpopulation of neurons with 380 nm light with the remaining neurons were kept in darkness. After treatment, AAQ was replaced with extracellular solution, whole-cell recordings were obtained, and photoresponsiveness was tested by applying alternating flashes of 380 and 500 nm light.

(b-c) Photoresponsiveness of neurons treated with AAQ either in 380 nm light **(b)** or in darkness **(c)**. Currents were elicited by stepping from -70 mV to $+30$ mV for 250 ms every 2 seconds while illuminating with 380 nm or 500 nm light. Recordings in **(b)** and **(c)** were from neurons on the same coverslip.

(d) Summary data showing average percent photoswitching of neurons treated with AAQ in 380 nm light or darkness ($n = 9-10$ neurons).

Figure 7. Photocontrol of action potential firing in intact circuits

(a) Rat cerebellar slices were treated with PAL and a loose-patch recording of spontaneous spiking was obtained from a cerebellar basket cell during alternating 360 nm light (violet) and 500 nm light (green). Basket cells were synaptically isolated from other neurons by using GABA and glutamate receptor antagonists.

(b) Simultaneous loose-patch recordings of bursting activity from the left and right heart interneurons (HN_L and HN_R) in the medicinal leech heartbeat CPG following PAL treatment and illumination as above.

(c) Loose-patch recording of PAL-mediated photoresponses in a rat RGC from a flat-mounted retina under alternating illumination.

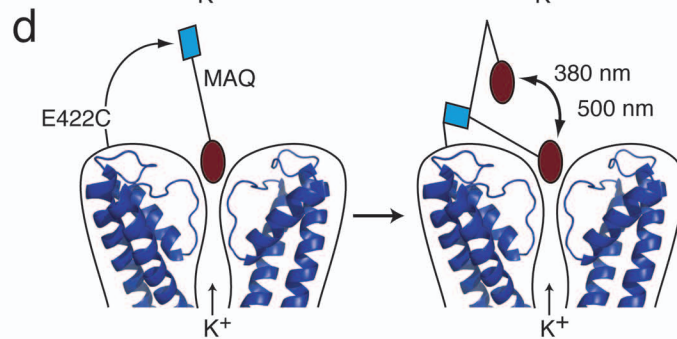
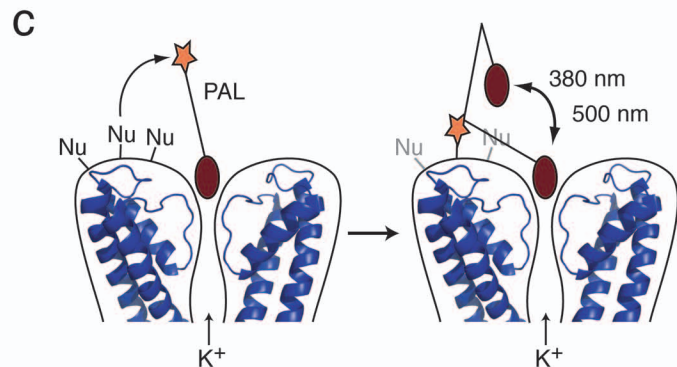
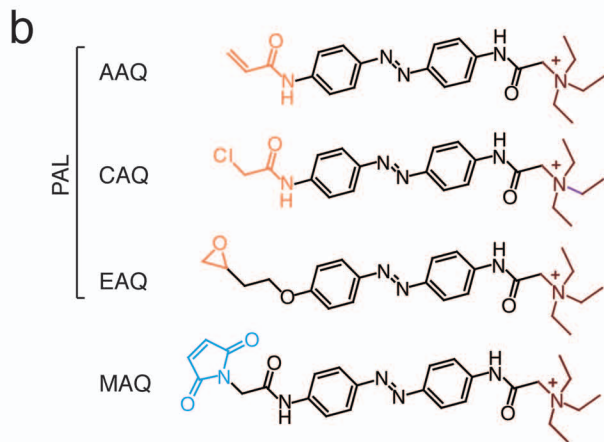
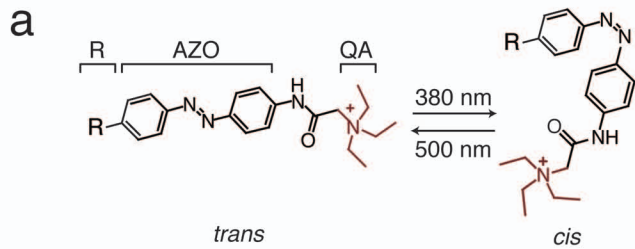
Supplementary Figure 1 Neuronal survival after PAL treatment

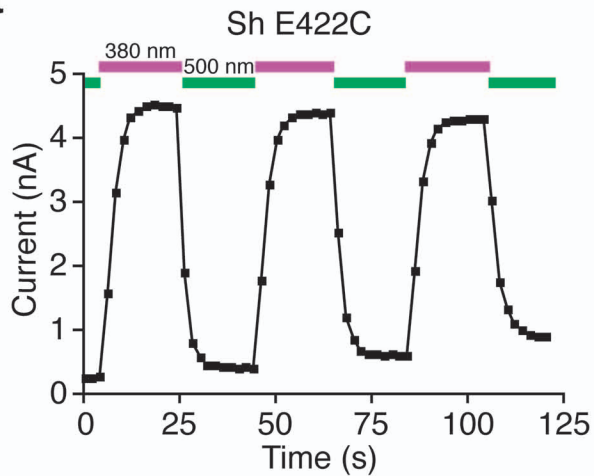
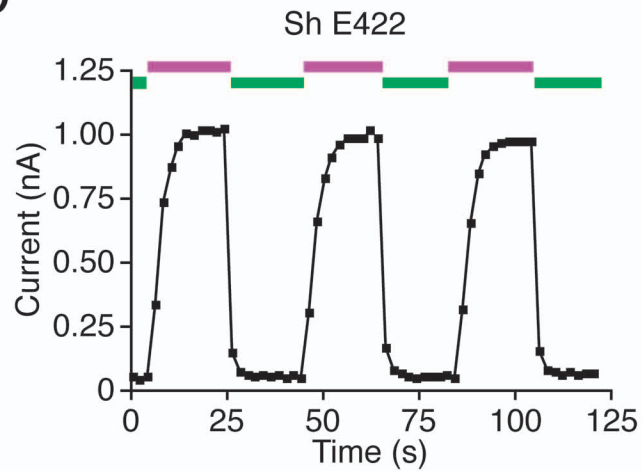
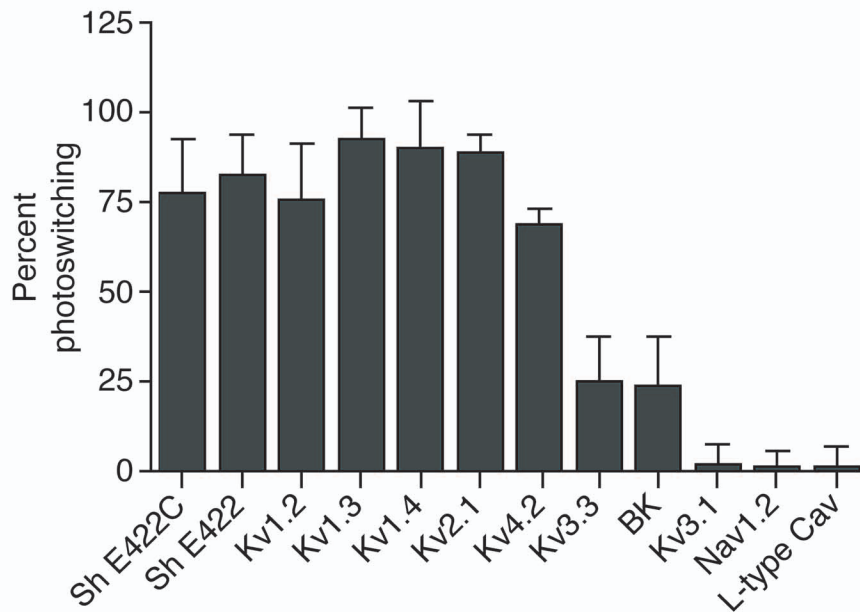
Supplementary Methods

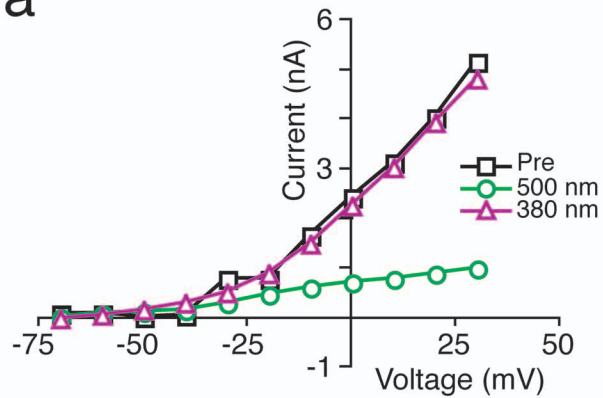
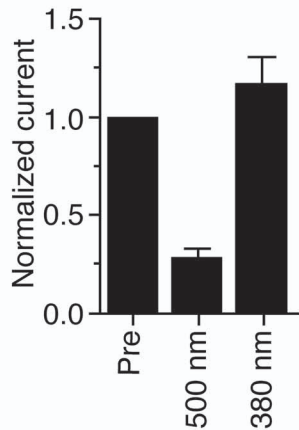
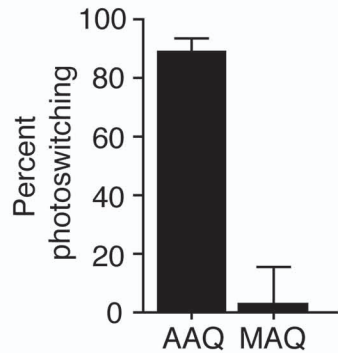
REFERENCES

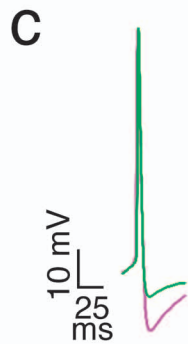
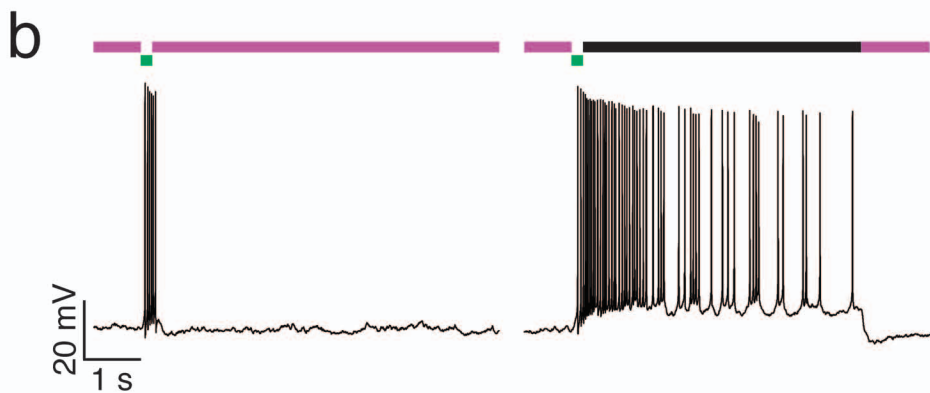
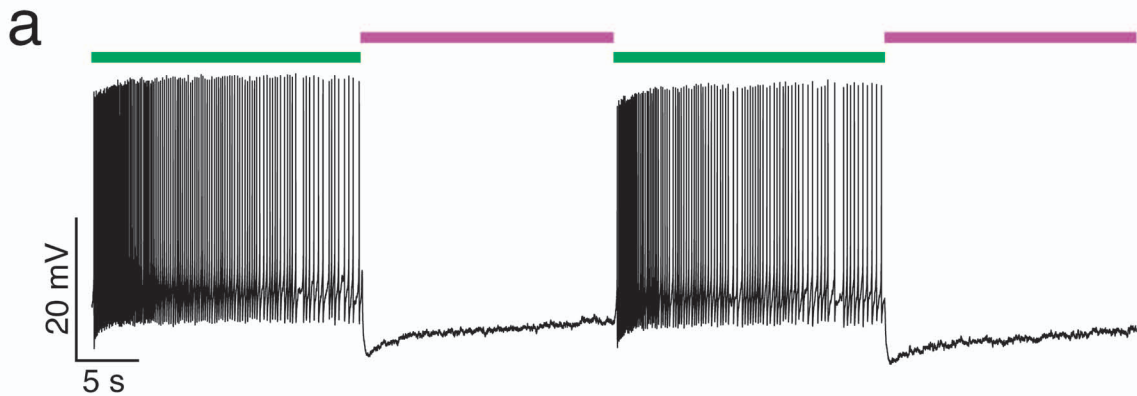
1. Callaway, E.M. & Yuste, R. Stimulating neurons with light. *Curr. Opin. Neurobiol.* **12**, 587-92 (2002).
2. Kramer, R.H., Chambers, J.J. & Trauner, D. Photochemical tools for remote control of ion channels in excitable cells. *Nat. Chem. Biol.* **1**, 360-5 (2005).
3. Miesenbock, G. & Kevrekidis, I.G. Optical imaging and control of genetically designated neurons in functioning circuits. *Annu. Rev. Neurosci.* **28**, 533-63 (2005).
4. Zhang, F., Wang, L.P., Boyden, E.S. & Deisseroth, K. Channelrhodopsin-2 and optical control of excitable cells. *Nat. Methods* **3**, 785-92 (2006).
5. Ellis-Davies, G.C. Caged compounds: photorelease technology for control of cellular chemistry and physiology. *Nat. Methods* **4**, 619-28 (2007).
6. Dalva, M.B. & Katz, L.C. Rearrangements of synaptic connections in visual cortex revealed by laser photostimulation. *Science* **265**, 255-8 (1994).
7. Callaway, E.M. & Katz, L.C. Photostimulation using caged glutamate reveals functional circuitry in living brain slices. *Proc. Natl. Acad. Sci. USA* **90**, 7661-5 (1993).
8. Shepherd, G.M., Pologruto, T.A. & Svoboda, K. Circuit analysis of experience-dependent plasticity in the developing rat barrel cortex. *Neuron* **38**, 277-89 (2003).
9. Nikolenko, V., Poskanzer, K.E. & Yuste, R. Two-photon photostimulation and imaging of neural circuits. *Nat. Methods* **4**, 943-50 (2007).
10. Banghart, M., Borges, K., Isacoff, E., Trauner, D. & Kramer, R.H. Light-activated ion channels for remote control of neuronal firing. *Nat. Neurosci.* **7**, 1381-6 (2004).
11. Volgraf, M. et al. Allosteric control of an ionotropic glutamate receptor with an optical switch. *Nat. Chem. Biol.* **2**, 47-52 (2006).
12. Szobota, S. et al. Remote control of neuronal activity with a light-gated glutamate receptor. *Neuron* **54**, 535-45 (2007).
13. Zhang, F. et al. Multimodal fast optical interrogation of neural circuitry. *Nature* **446**, 633-9 (2007).
14. Boyden, E.S., Zhang, F., Bamberg, E., Nagel, G. & Deisseroth, K. Millisecond-timescale, genetically targeted optical control of neural activity. *Nat. Neurosci.* **8**, 1263-8 (2005).
15. Bi, A. et al. Ectopic expression of a microbial-type rhodopsin restores visual responses in mice with photoreceptor degeneration. *Neuron* **50**, 23-33 (2006).
16. Li, X. et al. Fast noninvasive activation and inhibition of neural and network activity by vertebrate rhodopsin and green algae channelrhodopsin. *Proc. Natl. Acad. Sci. USA* **102**, 17816-21 (2005).
17. Han, X. & Boyden, E.S. Multiple-color optical activation, silencing, and desynchronization of neural activity, with single-spike temporal resolution. *PLoS ONE* **2**, e299 (2007).
18. Petreanu, L., Huber, D., Sobczyk, A. & Svoboda, K. Channelrhodopsin-2-assisted circuit mapping of long-range callosal projections. *Nat. Neurosci.* (2007).
19. Arenkiel, B.R. et al. In vivo light-induced activation of neural circuitry in transgenic mice expressing channelrhodopsin-2. *Neuron* **54**, 205-18 (2007).
20. Nagel, G. et al. Light activation of channelrhodopsin-2 in excitable cells of *Caenorhabditis elegans* triggers rapid behavioral responses. *Curr. Biol.* **15**, 2279-84 (2005).
21. Wang, H. et al. High-speed mapping of synaptic connectivity using photostimulation in

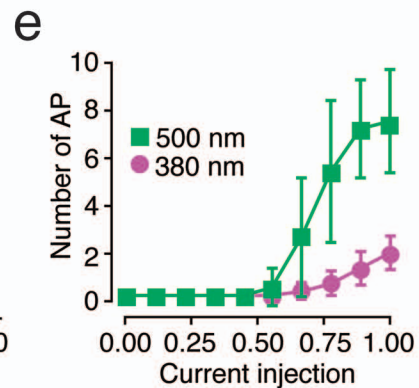
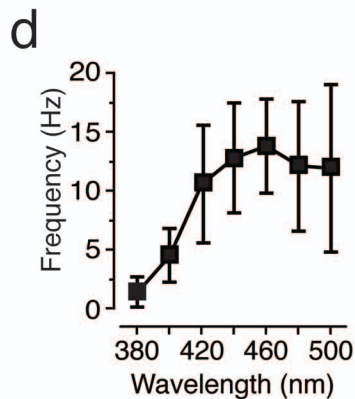
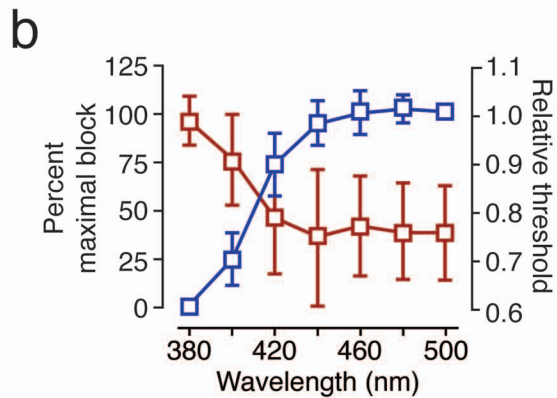
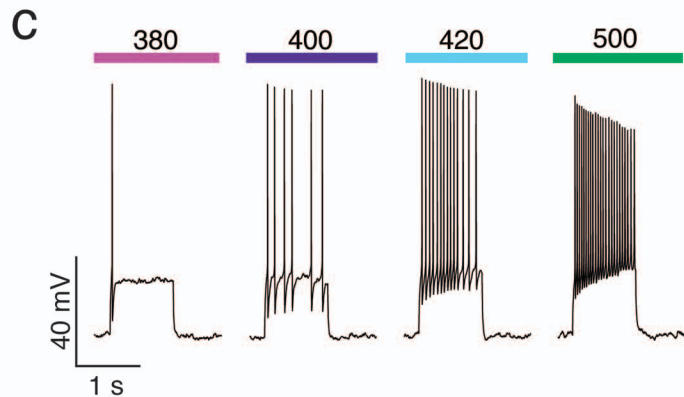
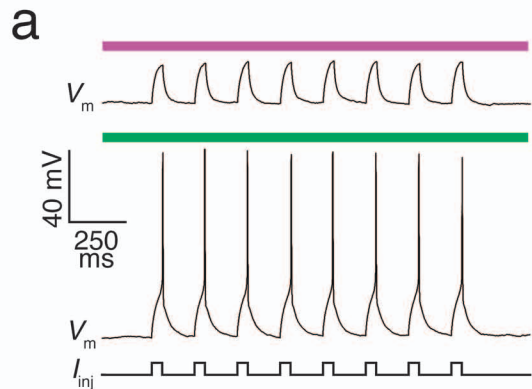
- Channelrhodopsin-2 transgenic mice. *Proc. Natl. Acad. Sci. USA* **104**, 8143-8 (2007).
22. Schroll, C. et al. Light-induced activation of distinct modulatory neurons triggers appetitive or aversive learning in *Drosophila* larvae. *Curr. Biol.* **16**, 1741-7 (2006).
 23. Wold, F. Affinity labeling--an overview. *Methods Enzymol.* **46**, 3-14 (1977).
 24. Gorostiza, P. et al. Mechanisms of photoswitch conjugation and light activation of an ionotropic glutamate receptor. *Proc. Natl. Acad. Sci. USA* **104**, 10865-70 (2007).
 25. Nadim, F. & Calabrese, R.L. A slow outward current activated by FMRFamide in heart interneurons of the medicinal leech. *J. Neurosci.* **17**, 4461-72 (1997).
 26. Hill, A.A., Lu, J., Masino, M.A., Olsen, O.H. & Calabrese, R.L. A model of a segmental oscillator in the leech heartbeat neuronal network. *J. Comput. Neurosci.* **10**, 281-302 (2001).
 27. Hattar, S., Liao, H.W., Takao, M., Berson, D.M. & Yau, K.W. Melanopsin-containing retinal ganglion cells: architecture, projections, and intrinsic photosensitivity. *Science* **295**, 1065-70 (2002).
 28. Laxhanpal, R.R. et al. Advances in the development of visual prostheses. *Curr. Opin. Ophthalmol.* **14**, 122-7 (2003).
 29. Xia, Z., Dudek, H., Miranti, C.K. & Greenberg, M.E. Calcium influx via the NMDA receptor induces immediate early gene transcription by a MAP kinase/ERK-dependent mechanism. *J. Neurosci.* **16**, 5425-36 (1996).
 30. Hoshi, T., Zagotta, W.N. & Aldrich, R.W. Biophysical and molecular mechanisms of Shaker potassium channel inactivation. *Science* **250**, 533-8 (1990).
 31. An, W.F. et al. Modulation of A-type potassium channels by a family of calcium sensors. *Nature* **403**, 553-6 (2000).
 32. Higgins, D. & Banker, G.A. Primary dissociated cell cultures. in *Culturing Nerve Cells* (eds. Banker, G.A. & Goslin, K.) (MIT Press, Cambridge, Massachusetts, 1998).
 33. Masino, M.A. & Calabrese, R.L. Phase relationships between segmentally organized oscillators in the leech heartbeat pattern generating network. *J. Neurophysiol.* **87**, 1572-85 (2002).

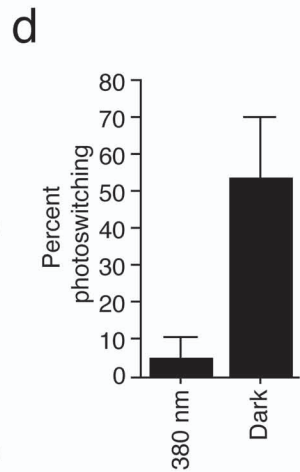
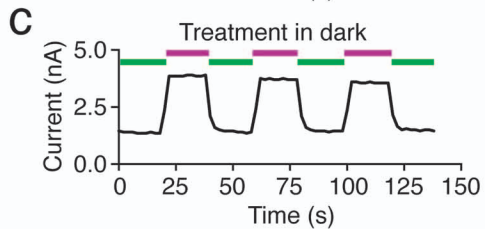
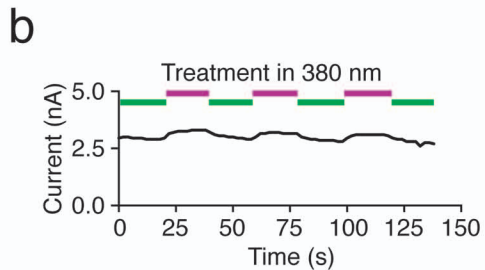
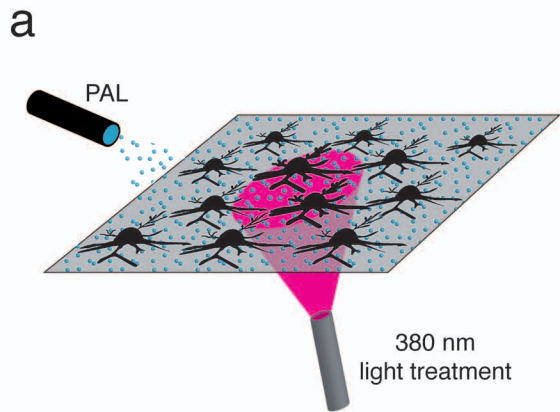


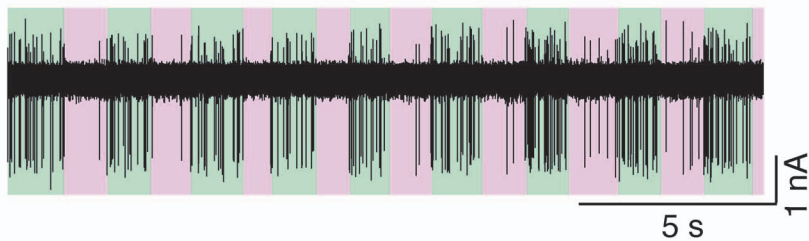
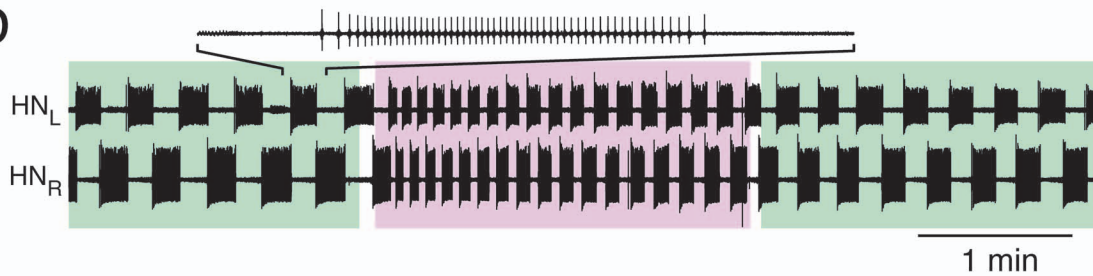
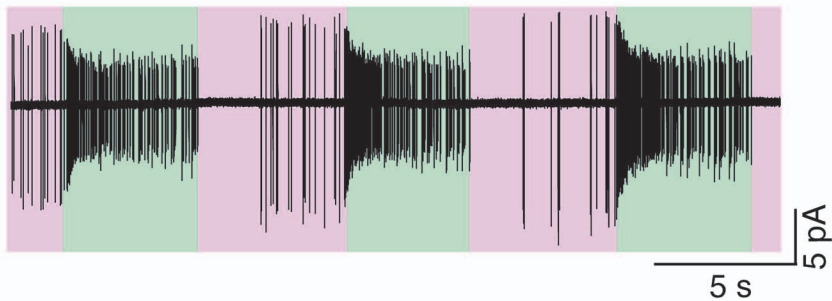
a**b****c**

a**b****c**



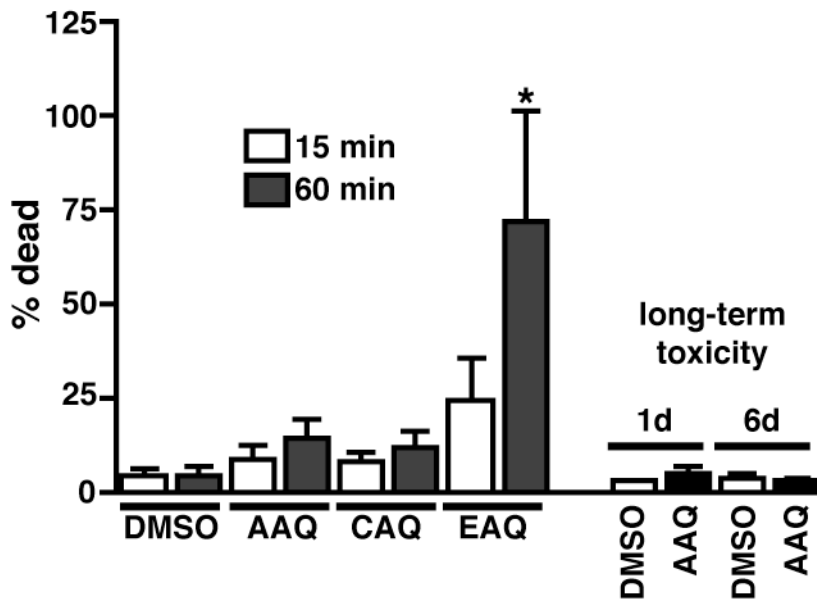




a**b****c**

Supplementary Figure 1. Neuronal survival after PAL treatment

Cultured hippocampal neurons were incubated with PALs for the indicated time and processed immediately after treatment for a Live/Dead Assay (Molecular Probes) to quantify cell survival. EAQ, but not AAQ and CAQ, caused more toxicity than vehicle alone (* $p < 0.001$ One-way ANOVA, Tukey's post-test). To assess long-term toxicity, neurons were treated with AAQ for 15 minutes then returned to their normal growth medium for an additional 1 or 6 days. AAQ treatment had no effect on long-term survival ($n = 4-8$ field of cells for each condition).



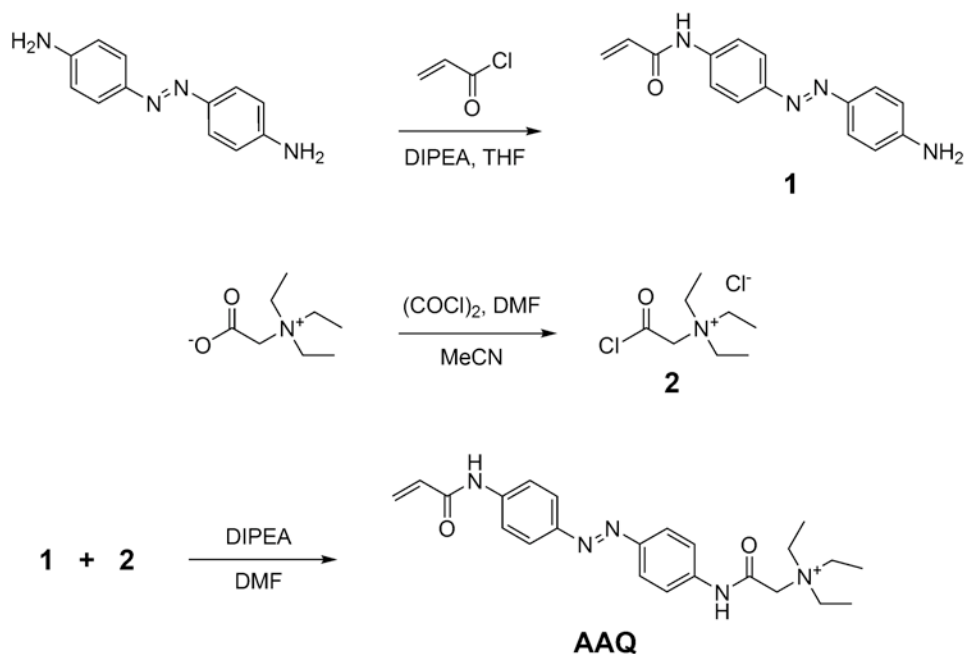
Supplementary methods

Electrophysiology. The bath solution for voltage-gated K^+ channel recordings contained in mM: 138 NaCl, 1.5 KCl, 1.2 $MgCl_2$, 2.5 $CaCl_2$, 5 HEPES, 10 glucose, pH 7.4 and when necessary, 20 μM bicuculline, 25 μM 6,7-dinitroquinoxaline-2,3-[1*H*,4*H*]-dione (DNQX) and 1 μM tetrodotoxin (TTX). The intracellular solution contained in mM: 10 NaCl, 135 K-gluconate, 10 HEPES, 2 $MgCl_2$, 2 MgATP, 1 EGTA, pH 7.4. For recordings of BK-mediated currents, 1 mM $CaCl_2$ was added to the intracellular solution. For recordings of voltage-gated Na^+ channels, the bath solution contained in mM: 150 NaCl, 2 $CaCl_2$, 0.5 $CdCl_2$, 10 HEPES, 5 glucose, pH 7.4; and the intracellular solution contained in mM: 100 CsCl, 30 NaCl, 10 EGTA, 1 $CaCl_2$, 2 $MgCl_2$, 2 ATP, 0.05 GTP, 10 HEPES, 5 glucose, pH 7.4. L-type calcium channel currents were recorded in a bath solution containing (in mM): 105 Tris-HCl, 0.8 $MgCl_2$, 5.4 KCl, 20 $BaCl_2$, 0.02 TTX, 10 HEPES, 5 glucose, pH 7.4. The intracellular solution contained (in mM): 70 Cs_2 -Aspartate, 20 HEPES, 11 EGTA, 1 $CaCl_2$, 5 $MgCl_2$, 5 glucose, 5 ATP, pH 7.4. Solutions were adjusted to 300-310 mOsm. Cerebellar slices recordings were performed in aCSF containing in mM: 119 NaCl, 26 $NaHCO_3$, 11 glucose, 2.5 KCl, 2.5 $CaCl_2$, 1.3 $MgCl_2$, and 1 NaH_2PO_4 and saturated with 95% O_2 and 5% CO_2 . RGC recording saline solution contained (in mM): 125 NaCl, 2.5 KCl, 2.5 $CaCl_2$, 1.5 $MgCl_2$, 1.25 NaH_2PO_4 , 33.7 $NaHCO_3$, and 10 glucose, pH 7.4.

General chemical methods. Reactions were carried out under N_2 atmosphere in flame-dried glassware. Tetrahydrofuran (THF) was distilled from Na/benzophenone immediately prior to use. Acetonitrile (MeCN), and diisopropylethylamine (DIPEA) were distilled from CaH_2 immediately prior to use. All other reagents and solvents were used without further purification from commercial sources. Flash column chromatography was carried out with EcoChrom ICN SiliTech 32–63 D 60 Å silica gel. Reverse-phase chromatography was carried out with Waters Preparative C18 Silica Gel WAT010001 125 Å and Waters Sep-Pak Vac 20 cc C18 Cartridges WAT036925. Reactions and chromatography fractions were monitored with either Merck silica gel 60F254 plates or Analtech C18 silica gel RPS-F 52011 plates, and visualized with 0.1N HCl. NMR spectra were measured in specified solvents and calibrated from residual solvent signal on a Bruker DRX spectrometer at 500 MHz for 1H spectra and 125 MHz for ^{13}C spectra and either a

Bruker AVB or Bruker AVQ spectrometer at 400 MHz for ^1H spectra and 100 MHz for ^{13}C spectra. IR spectra were measured with a Genesis FT-IR spectrometer by thin film.

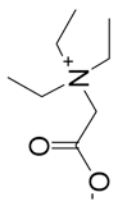
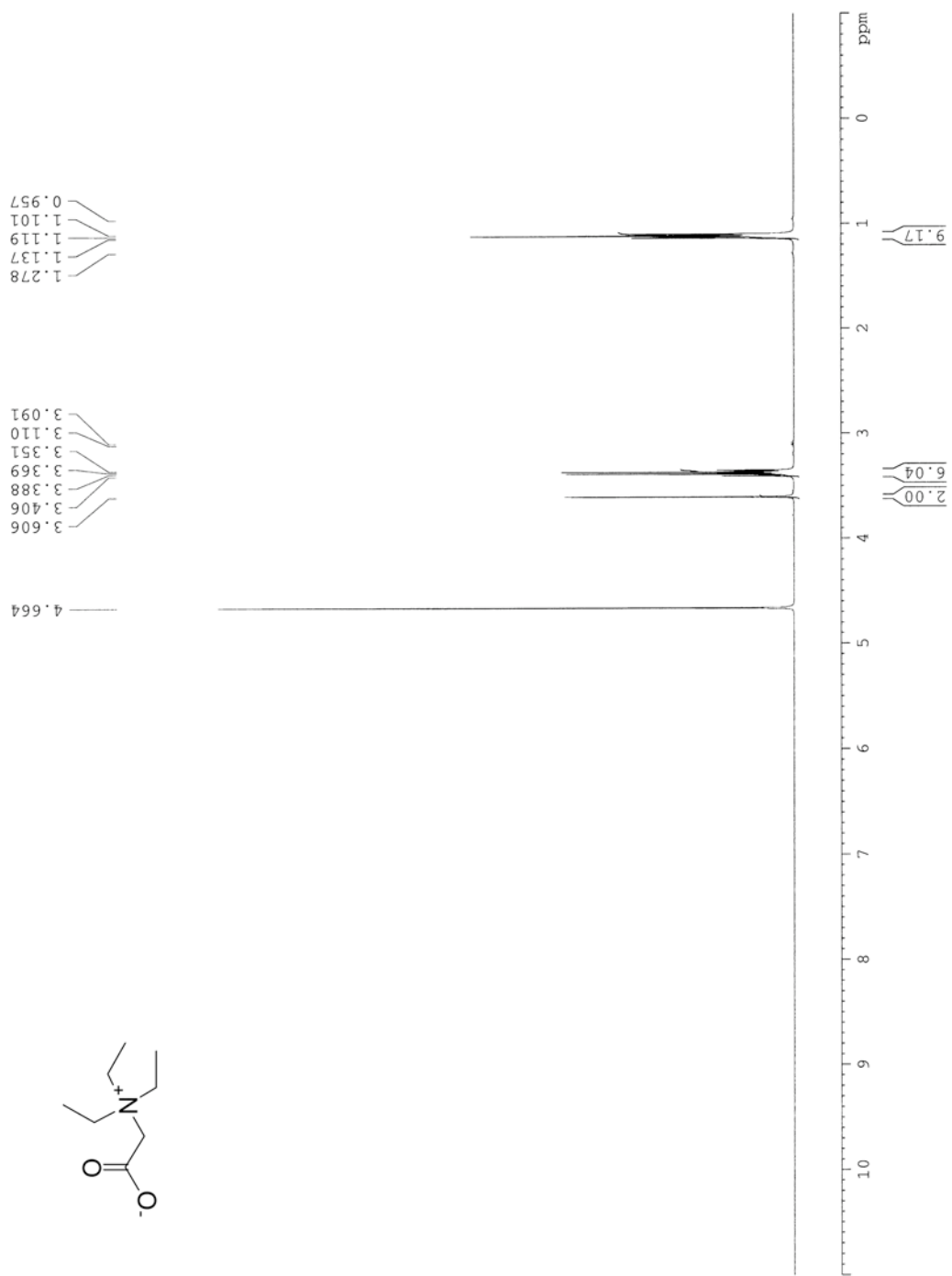
Scheme for synthesis of AAQ

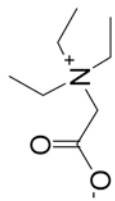
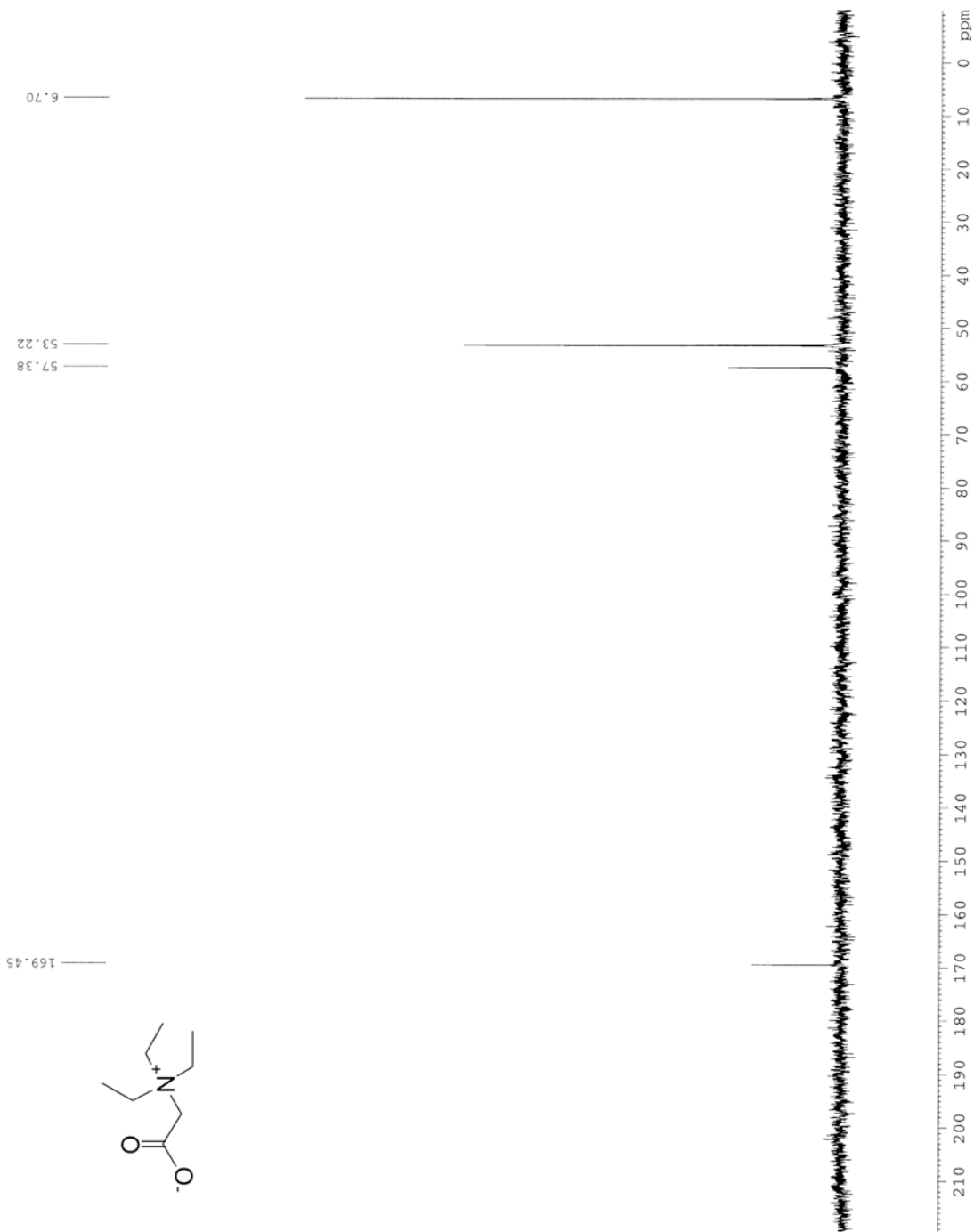


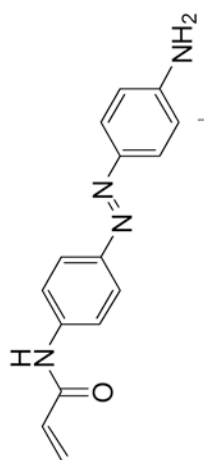
4-acrylamido-4'-aminoazobenzene (1). To a solution of 4,4'-diaminoazobenzene **2** (200 mg, 0.94 mmol) and DIPEA (0.1 ml, 0.56 mmol) in THF (300 ml) at 0°C was added acryloyl chloride (0.04 ml, 0.47 mmol) in THF (5 ml) over 1 h. The reaction was stirred for 15 min, warmed to room temperature and stirred for 1 h, at which time the crude mixture was removed of solvent *in vacuo* and immediately dry loaded onto silica gel (2 g). Silica gel chromatography through a wide column (10% EtOAc in DCM gradient to 75%) provided 4-acrylamido-4'-azobenzene as an orange solid (91 mg, 0.34 mmol, 72% yield): ^1H (CD_3CN , 300MHz): 4.77 (s, 2H); 5.74-5.78 (m, 1H); 6.36-6.38 (m, 2H); 6.73 (d, 2H, $J=8.7$); 7.70 (d, 2H, $J=8.7$); 7.79 (s, 4H); 8.66 (s, 1H). ^{13}C (CD_3CN , 125MHz): 114.9, 120.8, 123.7, 125.7, 127.9, 132.4, 141.3, 145.3, 149.9, 152.5, 164.5. IR (thin film): 2925, 1671, 1598, 1536, 1244. HRMS (FAB+): calculated for $\text{C}_{15}\text{H}_{15}\text{N}_4\text{O}$ – 267.1256, found – 267.1246 (M+). The remaining 4,4'-azodiaminoazobenzene was isolated for reuse.

2-triethylammonium acetic acid chloride chloride (2). Triethylammonium acetate was prepared as described previously¹. ¹H (D₂O, 400MHz): 1.12 (t, 9H, J=7.2); 3.38 (q, 6H, J=7.2); 3.61 (s, 2H). ¹³C (D₂O, 100MHz): 6.7, 53.2, 57.4, 169.5. IR (thin film): 1626, 1458, 1395. HRMS (ESI+): calculated for C₈H₁₈NO₂ – 160.1338, found – 160.1341 (MH+). To a solution of triethylammonium acetate (520 mg, 3.25 mmol) in MeCN (3 ml) was added a 2 M solution of oxallyl chloride in DCM (1.6 ml, 3.25 mmol) followed by several drops of DMF. The solution was stirred at ambient temperature for 15 min, removed of solvent *in vacuo* and dried under vacuum for 1 hr to remove residual HCl. The product was then taken up in DMF (10 ml) and used without further purification.

Acryl-Azo-QA (AAQ) (3). To a solution of 4-acrylamido-4'-aminoazobenzene **1** (90 mg, 0.33 mmol) and DIPEA (0.12 ml, 0.66 mmol) in DMF (5 ml) at 0°C was added 2-triethylammonium acetic acid chloride chloride **2** (0.41 mmol) in DMF and stirred for 15 min, then warmed to ambient temperature and stirred for 1 h at which time the solvent was removed *in vacuo*. Reverse phase silica gel chromatography (0.1% formic acid in H₂O to 50% MeCN: 0.1% formic acid in H₂O) provided **AAQ** as an orange solid (109 mg, 0.24 mmol, 70% yield): ¹H (CD₃CN, 400MHz): 1.30 (t, 9H, J=7.2); 3.52 (q, 6H, J=7.2); 4.47 (s, 2H); 5.72-5.75 (m, 1H); 6.33-6.38 (m, 1H); 6.54-6.61 (m, 1H); 7.75-7.79 (m, 4H); 7.87-7.90 (m, 4H); 8.72 (s, 1H); 10.21 (s, 1H); 12.88 (s, 1H). ¹³C (CD₃CN, 100MHz): 8.1, 55.4, 57.7, 120.8, 121.4, 124.2, 124.3, 127.6, 132.8, 142.1, 143.0, 149.3, 149.7, 163.4, 154.9, 168.1. IR (thin film): 2986, 1684, 1594, 1541, 1250. HRMS (FAB+): calculated for C₂₃H₃₀N₅O₂ – 408.2400, found – 408.2395 (M+).







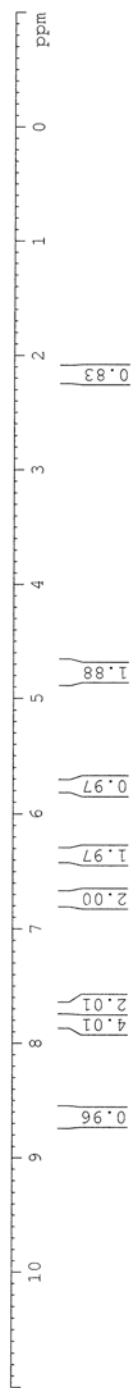
2.165
1.967
1.951
1.943
1.935
1.927
1.919
1.254
1.221
1.197
1.174
0.848

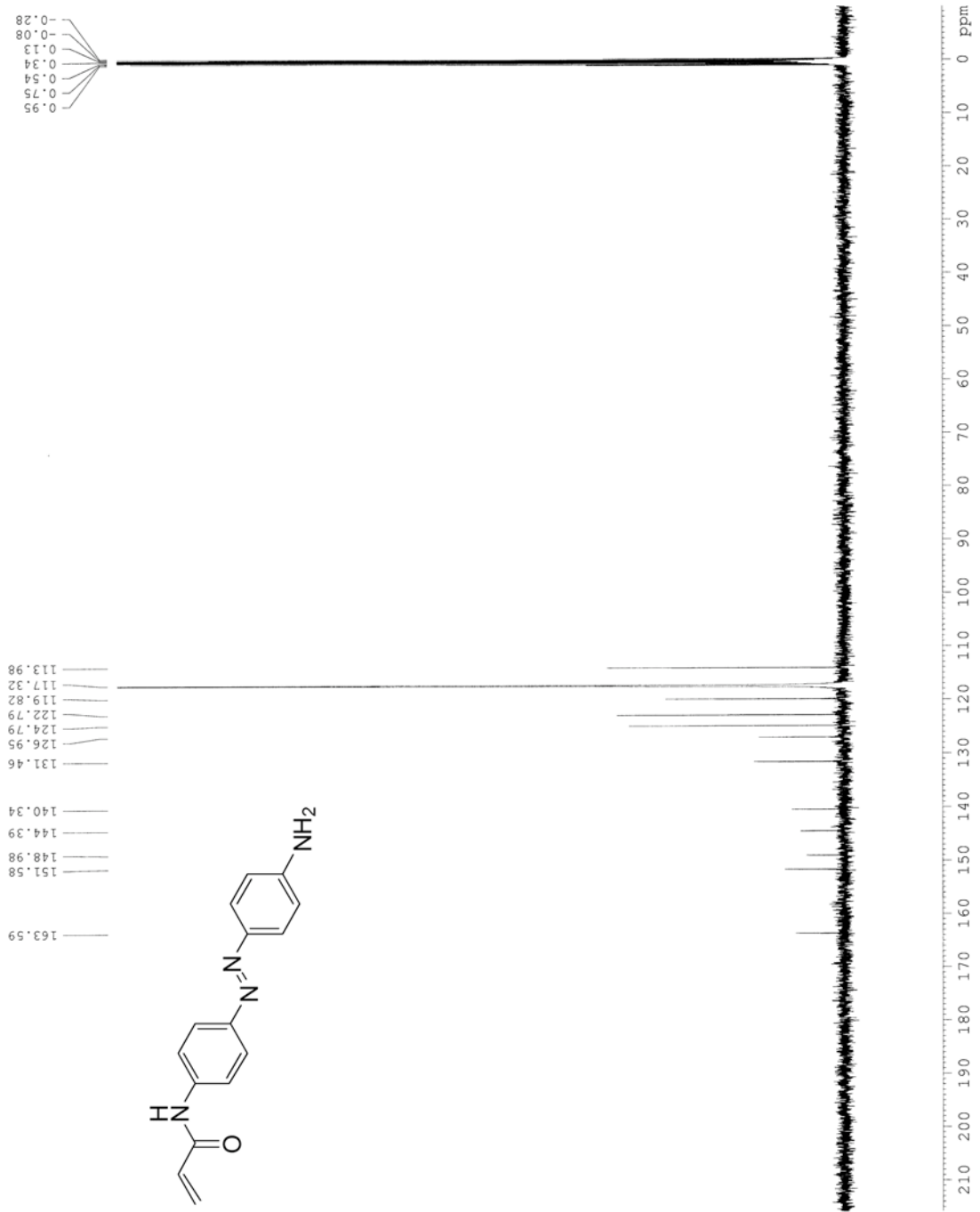
4.064
4.041

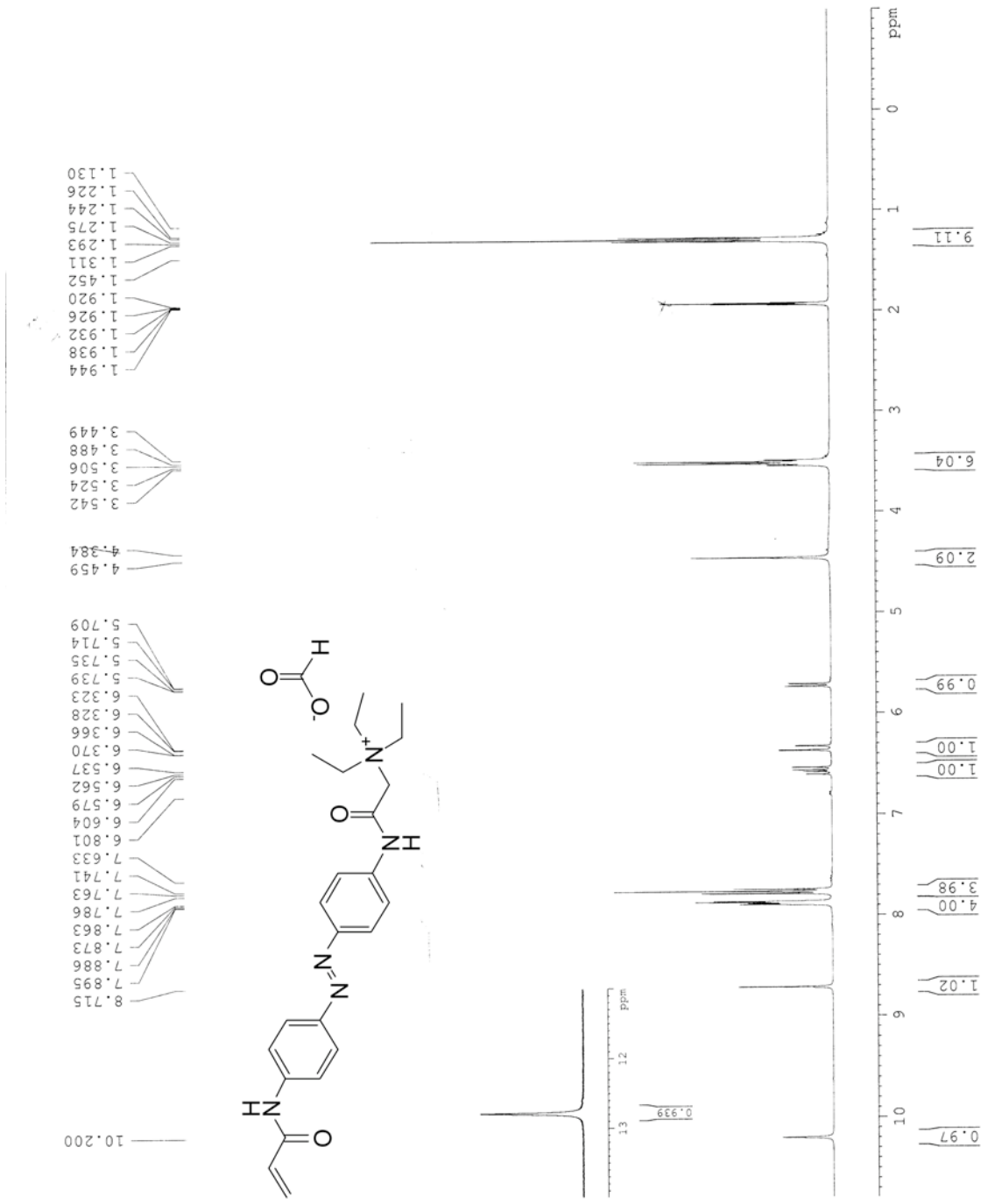
4.769

5.739
5.755
5.764
5.779
6.314
6.355
6.370
6.380
6.436
6.718
6.747

7.789
7.713
7.684



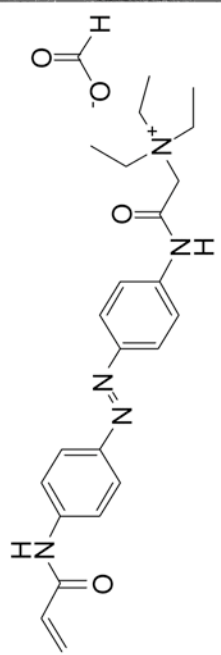




7.09
0.91
0.71
0.50
0.29
0.09
-0.12
-0.33

56.72
54.41

167.17
163.90
162.44
148.77
148.28
142.03
141.09
131.79
126.67
123.37
123.27
120.45
119.87
117.29



210 200 190 180 170 160 150 140 130 120 110 100 90 80 70 60 50 40 30 20 10 0 ppm

References

1. Challenger, F.; Taylor, P.; Taylor, B. *Journal of the Chemical Society, Abstracts* **1942**, 48-55.